

Low-energy hadronic cross sections measurements at BABAR and $g - 2$ of the muon

Denis Bernard,

LLR, Ecole Polytechnique, CNRS/IN2P3, 91128 Palaiseau, France

On behalf of the *BABAR* Collaboration

October 22, 2018

Abstract

Even though the standard model of particle physics has been tested in depth by several generations of researchers and has been found to be completely standard, some hints of new physics are cropping out here and there, most notably the long-pending 3-ish standard deviation discrepancy between the predictions and the measurement of the muon anomalous magnetic moment a_μ . The experimental information originates from one single precise measurement, while the prediction uncertainty is dominated by two main contributions, the hadronic vacuum polarization (VP) modification of the photon propagator and the hadronic light-by-light scattering (LbL). The leading-order (LO) VP contribution to a_μ is obtained using the dispersion relation and the optical theorem as the integral as a function of energy of an expression that involves the ratio of the $e^+e^- \rightarrow$ hadrons cross section to the pointlike muon pair cross section. The former is extracted from experimental data for individual hadronic final states at low energies, and from perturbative QCD at high energies.

The *BABAR* experiment at SLAC has a programme of systematic measurement of the production of the lowest-rest-mass hadronic final states, those that contribute most significantly to the integral. To that purpose, we use a method in which, while the PEP-II storage ring is operated at a constant energy in the center of mass system, \sqrt{s} , of about 10.6 GeV, events are reconstructed and selected which have been produced with a hadronic final state together with a high-energy photon which may (photon tagging) or may not (no tagging) be observed. In our kinematic configuration the photon is almost always emitted by the electron or by the positron of the initial state, hence the name “initial-state radiation” (ISR). The cross section for the direct $e^+e^- \rightarrow f$ production of a final state f at an energy $\sqrt{s'}$ is then extracted from the differential cross section of the ISR production of the state f with invariant mass $\sqrt{s'}$. The programme is almost completed and has led to a number of first measurements and to an improvement of up to a factor of three of the uncertainties on the contributions of individual channels to a_μ . The uncertainty on a_μ^{VP} is now of similar magnitude as that on a_μ^{LbL} .

On the experimental side, two projects aiming at a measurement of a_μ with an improved precision are in preparation at Fermilab and at J-PARC: their results are eagerly awaited !

Talk given at QCD 16, 19th International Conference in Quantum Chromodynamics, 4 - 8 July 2016, Montpellier - France

1 The muon gyromagnetic factor and “anomalous” moment

As a result of more than three decades of intense efforts to validate every corner of the standard model (SM) of elementary particles and their interactions, and to submit it to a redundant metrology with an always increasing precision, the SM has only become more and more “standard”, with some very few exceptions that include the “tension” between the theoretical prediction and the unique precise experimental measurement of the “anomalous” magnetic moment of the muon, a_μ , which is the relative deviation of the gyromagnetic factor, g_μ , from the value of $g = 2$ for a pointlike Dirac particle, i.e. $a_\mu \equiv (g_\mu - 2)/2$.

2 a_μ : predictions and measurement

Since the first measurement (for the electron) [1] and its interpretation within the QED framework [2], both the prediction and the measurement of a have undergone a tremendous improvement in precision, to the point that hadronic vacuum polar-

ization (VP) i.e. modifications of the photon propagator, hadronic light-by-light scattering (LbL) and weak interactions must be taken into account (Fig. 1). Understanding the value of a_μ necessi-

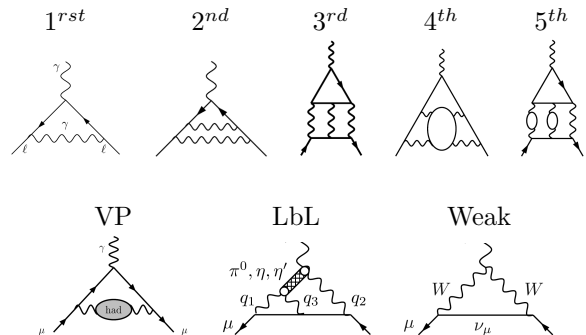


Figure 1: Examples of diagrams contributing to the calculation of a_μ . Top: QED diagrams of various orders in α . Bottom: Hadronic Vacuum Polarisation (VP), Hadronic light-by-light scattering (LbL) and weak-interaction contributions [10].

itates a precise knowledge of the value of the fine structure constant α . From the development [3] of a_e and of a_μ (I have truncated the numerical factors),

$$a_e = \frac{\alpha}{2\pi} - 0.3 \left(\frac{\alpha}{\pi}\right)^2 + 1.2 \left(\frac{\alpha}{\pi}\right)^3 - 1.9 \left(\frac{\alpha}{\pi}\right)^4 + 9.2 \left(\frac{\alpha}{\pi}\right)^5 + 1.7 \times 10^{-12}(\text{QCD} + \text{weak}),$$

$$a_\mu = \frac{\alpha}{2\pi} + 0.8 \left(\frac{\alpha}{\pi}\right)^2 + 24. \left(\frac{\alpha}{\pi}\right)^3 - 131. \left(\frac{\alpha}{\pi}\right)^4 + 753. \left(\frac{\alpha}{\pi}\right)^5 + 7.1 \times 10^{-8}(\text{QCD} + \text{weak}),$$

we see that due to the μ -to- e mass difference, the development for a_e converges extremely rapidly and that the non-QED contributions are very small: a precise value of α can be extracted from a_e and then injected in the calculation of a_μ . The value of a_μ so obtained has a very small uncertainty and is compatible with that obtained using a value of α from atomic physics (Table 1): the QED contribution, which has been computed up to the 5th order in α [3], is under excellent control. Table 2 presents the sizable contributions to the prediction and the comparison with experiment as of 2014 [4]:

- The QED contribution is the main contributor to the value of a_μ , while the uncertainty

Table 1: Values of a_μ^{QED} computed using values of α extracted from the measured value of a_e and from atomic physics measurements [3].

α from	$a_\mu^{\text{QED}} (10^{-10})$
a_e	11 658 471.885 \pm 0.004
Rubidium Rydberg constant	11 658 471.895 \pm 0.008

is dominated by the hadronic contributions (VP and LbL);

- The uncertainties of the prediction and of the measurement are of similar magnitude;

Table 2: Contributions to the prediction for a_μ (10^{-10}) and comparison with experiment as of 2014 [4].

QED	11 658 471.895	± 0.008
Leading hadronic vacuum polarization (VP)	692.3	± 4.2
Sub-leading hadronic vacuum polarization	-9.8	± 0.1
Hadronic light-by-light (LbL)	10.5	± 2.6
Weak (incl. 2-loops)	15.4	± 0.1
Theory	11 659 180.3	$\pm 4.2 \pm 2.6$
Experiment (E821 @ BNL) [5]	11 659 209.1	$\pm 5.4 \pm 3.3$
Exp. - theory	+28.8	± 8.0

- The measured value exceeds the prediction with, assuming Gaussian statistics, a significance of ≈ 3.6 standard deviations.

As QCD is not suited to precise low energy calculations, the VP contribution to a_μ is computed from the “dispersion integral” ([10] and references therein):

$$a_\mu^{\text{VP}} = \left(\frac{\alpha m_\mu}{3\pi} \right)^2 \int \frac{R(s) \times \hat{K}(s)}{s^2} ds, \quad (1)$$

where $R(s)$ is the the cross section of e^+e^- to hadrons at center-of-mass (CMS) energy squared s , normalized to the pointlike muon pair cross section σ_0 : $R(s) = \sigma_{e^+e^- \rightarrow \text{hadrons}}/\sigma_0$, and $\hat{K}(s)$ is a known function that is of order unity on the s range $[(2m_\pi c^2)^2, \infty[$. Technically, the low energy part of the integral is obtained from experimental data (up to a value often chosen to be $E_{\text{cut}} = 1.8 \text{ GeV}$), while the high-energy part is computed from perturbative QCD (pQCD). Due to the presence of the s^2 factor at the denominator of the integrand, the precision of the prediction of a_μ relies on precise measurements at the lowest energies, and the channels with the lightest final state particle rest masses, $\pi^+\pi^-$, $\pi^+\pi^-\pi^0$, $\pi^+\pi^-2\pi^0$, $\pi^+\pi^-\pi^+\pi^-$, KK are of particular importance.

3 BABAR measurements: the ISR method

The *BABAR* experiment [27, 28] at the SLAC National Accelerator Laboratory has committed itself over the last decade to the systematic measurement of the production of all hadronic final

states using the initial-state radiation (ISR) process. The cross section of the e^+e^- production of a final state f at a CMS energy squared s' can be obtained from the differential cross section of the ISR production $e^+e^- \rightarrow f \gamma$ through the expression:

$$\frac{d\sigma_{[e^+e^- \rightarrow f \gamma]}(s')}{ds'} = \frac{2m}{s} W(s, x) \sigma_{[e^+e^- \rightarrow f]}(s'), \quad (2)$$

where $W(s, x)$, the probability density to radiate a photon with energy $E_\gamma = x\sqrt{s}$, is a known “radiator” function [6], and \sqrt{s} is here the CMS energy of the initial e^+e^- pair, which is close to 10.6 GeV for *BABAR*. In contrast with the energy scans that provided the earlier experimental information on the variations of R (see Figs. 50.5 and 50.6 in Ref. [4] and references in their captions), this ISR method makes an optimal use of the available luminosity and allows a consistent measurement over the full energy range with the same accelerator and detector conditions. In addition, in the case of *BABAR* the e^+e^- initial state is strongly boosted longitudinally so the detector acceptance stays sizable down to threshold (Fig. 2 top).

The observation of the hadronic final state alone, if kinematically compatible with a system recoiling against a single massless particle, would allow the reconstruction of the event and the measurement of s' , but when in addition the ISR photon is observed (γ -tagging), a powerful background rejection and a good signal purity can be achieved.

We have performed most of these measurements using a leading-order (LO) method, in which the final state f and the ISR photon are reconstructed

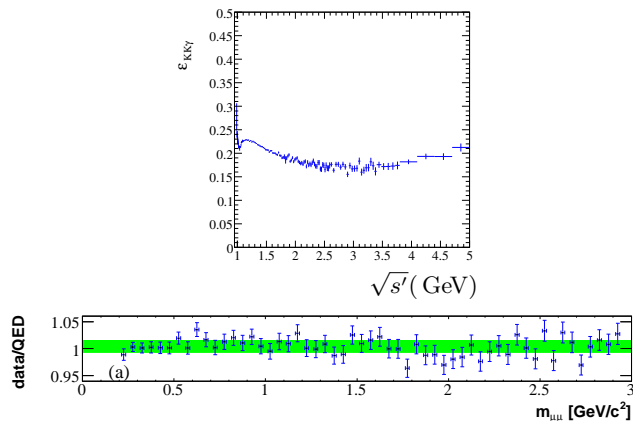


Figure 2: Bottom: $\mu^+\mu^-$ cross section as a function of the $\mu^+\mu^-$ invariant mass compared to the QED prediction, as a sanity check for the *BABAR* NLO analyses [34–36]. Top: The *BABAR* acceptance for the K^+K^- analysis as a function of the K^+K^- invariant mass [36].

regardless of the eventual presence of additional photons. For these analyses the ISR differential luminosity is obtained from the luminosity of the collider, which is known with a typical precision of 1%, and involves a computation of the detection efficiency that relies on Monte Carlo (MC) simulations¹ [29–33], [38–44]. This experimental campaign has lead *BABAR* to improve the precision of the contribution to a_μ^{VP} of most of the relevant channels by a large factor, typically close to a factor of three.

A list of the contributions a_μ^f to a_μ^{VP} for a number of individual hadronic final states f , available at the time, can be found in Table 2 of Ref. [13].

4 BaBar NLO ($e^+e^- \rightarrow f \gamma (\gamma)$) results

BABAR has also developed a method that we applied to the dominant channel $\pi^+\pi^-$ [34, 35] and more recently to the K^+K^- channel [36]. The control of the systematics below the % level made it necessary to perform the analysis at the NLO level, that is, to take into account the possible radiation of an additional photon, be it from the initial (ISR) or from the final (FSR) state. The im-

¹ A review on the *PHOKHARA* and *AfKQED* event generators used in our *GEANT4*-based simulations can be found in section 21 of Ref. [7].

possibility to control the global differential luminosity with the desired precision, in particular the MC-based efficiency, lead us to derive the value of R from the ratio of the ISR production of the final state f to the ISR production of a pair of muons, $\mu^+\mu^-$. Most of the systematics, including those related to the absolute luminosity, of the ISR photon reconstruction and of additional ISR radiation, cancel in the ratio. Figure 3 shows the obtained form-factor (here squared) distributions extracted from the cross-section distributions, together with fits using the GS parametrization of the VDM model. The values of $a_\mu^{\pi^+\pi^-}$ and of

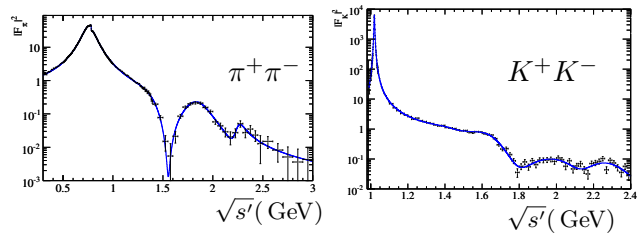


Figure 3: *BABAR* NLO measurements: Vector dominance model (VDM) fits of the squared form-factors using a Gounaris-Sakurai (GS) parametrization. Left: $\pi^+\pi^-$ [34, 35]. Right: K^+K^- [36].

$a_\mu^{K^+K^-}$ integrated over the most critical range, that is, from threshold to 1.8 GeV are more precise than the average of the previous measurements (Table 3).

Even though neither the time-integrated luminosity nor the absolute acceptance/efficiency were used in these precise $\pi^+\pi^-$ and K^+K^- cross-section measurements, we checked that we understand them by comparing the $\mu^+\mu^-$ cross section distribution we observe to the QED prediction: a good agreement is found (Fig. 2 bottom) within $0.4 \pm 1.1\%$, which is dominated by the uncertainty on the time-integrated luminosity ($\pm 0.9\%$).

These NLO analyses were performed assuming that the FSR corrections for the hadronic channel are negligible, as theoretical estimates are well below the systematic uncertainties in the cross section [34–36]. We have validated this assumption by an experimental study of the ISR-FSR interference in $\mu^+\mu^-$ and $\pi^+\pi^-$ ISR production. Because charge parities of the final state pair are opposite for ISR and FSR, the interference be-

Table 3: Contributions to a_μ^{VP} for recent *BABAR* publications: comparison of the measured value to the previous world average on the energy range $\sqrt{s'} < 1.8$ GeV (units 10^{-10}).

	$\pi^+\pi^-$	$\pi^+\pi^-\pi^+\pi^-$	K^+K^-
<i>BABAR</i>	$514.1 \pm 2.2 \pm 3.1$ [34, 35]	$22.93 \pm 0.18 \pm 0.22 \pm 0.03$ [38]	$13.64 \pm 0.03 \pm 0.36$ [36]
Previous average [13]	503.5 ± 4.5	$21.63 \pm 0.27 \pm 0.68$	$13.35 \pm 0.10 \pm 0.43 \pm 0.29$
Their difference Δ	$+10.6 \pm 5.9$	$+1.30 \pm 0.79$	$+0.29 \pm 0.63$

tween ISR and FSR changes sign with the charge interchange of the two muons (pions). As a consequence, investigation of the charge asymmetry of the process gives access to the interference between ISR and FSR, which enables the separate measurement of the magnitudes of the ISR and of the FSR amplitudes [37]. For the pion channel, results match a model where final state radiation originates predominantly from the quarks that subsequently hadronize into a pion pair, while for the muon control channel, good consistency is found with QED.

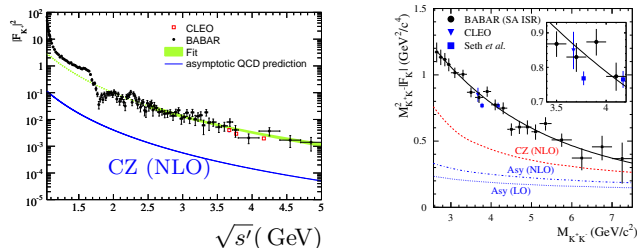


Figure 4: Comparison of the *BABAR* K^+K^- results with Chernyak-Zhitnitsky (CZ) [8] pQCD predictions. With (left, [36]) and without (right, [44]) γ tagging.

5 Recent BaBar LO ($e^+e^- \rightarrow f \gamma$) results

Recently *BABAR* obtained results on channels with two neutral kaons $K_S^0 K_L^0$, $K_S^0 K_L^0 \pi^+ \pi^-$, $K_S^0 K_S^0 \pi^+ \pi^-$ and $K_S^0 K_S^0 K^+ K^-$ [42] (Fig. 5 top), on $K_S^0 K^+ \pi^- \pi^0$ and $K_S^0 K^+ \pi^- \eta$ (preliminary) (Fig. 5 bottom), and updated the $p\bar{p}$ analysis to the full statistics [43] (Fig. 5 center left). The $p\bar{p}$ measurement has also been extended up to 6.5 GeV [40] (Fig. 5 center center) and the K^+K^- measurement to 8 GeV [44] (Fig. 5 center right) by untagged analyses.

pQCD is found to fail to describe the K^+K^- form factors extracted from our cross section measurements (Fig. 4), but there is some hint that

the discrepancy is getting better at higher mass, which kind-of supports the use of pQCD for the calculation of the dispersion integral above E_{cut} . Note that given the improvement in precision of the hadronic cross sections, the most recent prediction [16] restricts the s range over which pQCD is used to [4.5 – 9.3] GeV and [13 GeV – ∞].

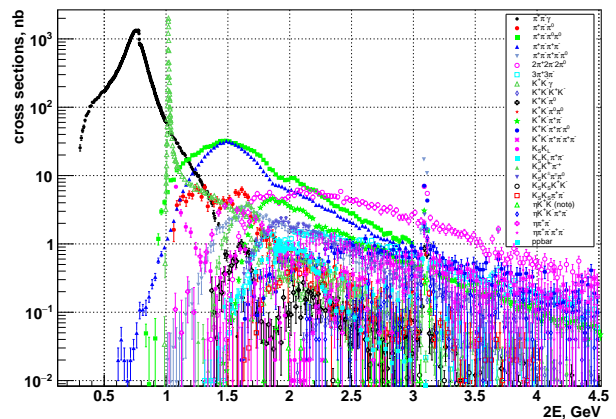


Figure 6: Summary of the *BABAR* measurements (Courtesy of Fedor V. Ignatov, April 2016). Beware that some channels have the charmonia contribution removed while some others have not. The $\pi^+\pi^-\pi^0\pi^0$ [41] and $K_S^0 K^+ \pi^- \pi^0$ [41] entries are preliminary. NLO measurements are denoted by an additional “ γ ”.

A summary of the *BABAR* measurements is provided in Fig. 6 and Table 4. The analyses of the $\pi^+\pi^-\pi^0\pi^0$ [41], of the $\pi^+\pi^-\pi^0$ [29] and of the $\pi^+\pi^-\eta$ [32] channels are presently being updated with the full available statistics: stay tuned.

The methods used by various experiments for the $\pi^+\pi^-$ channel are listed in Table 5 and their results shown in Fig. 8.

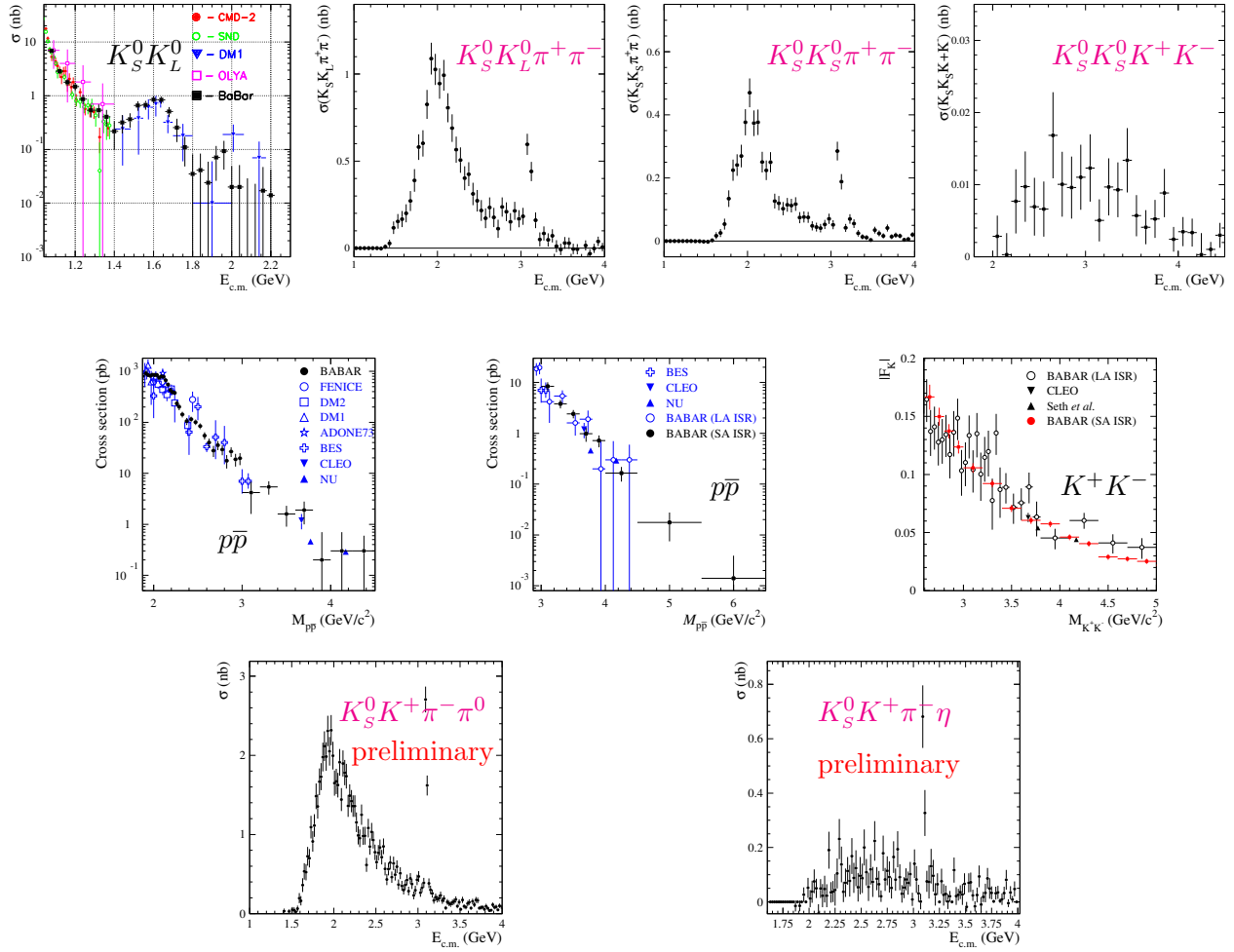


Figure 5: Recent LO results. **Magenta: First measurements.** Top: channels with two neutral kaons [42]. Center: $p\bar{p}$ with [43] and without [40] γ tagging, and K^+K^- without [44] γ tagging. Bottom: $K_S^0 K^+ \pi^- h^0$, the neutral meson h^0 being either a π^0 or an η (preliminary).

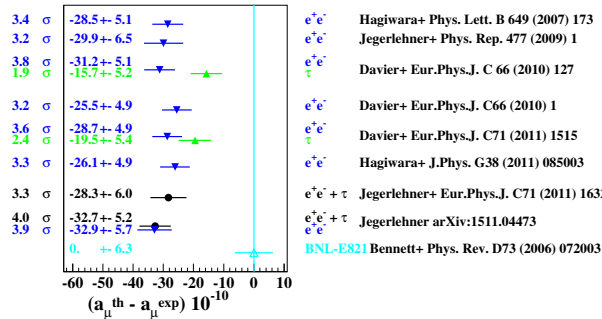


Figure 7: Predictions of the value of a_{μ} [9–16] after the experimental value (Cyan) [5] is subtracted. **Blue:** e^+e^- -based; **Green:** τ spectral function-based; **Black:** e^+e^- and τ combinations.

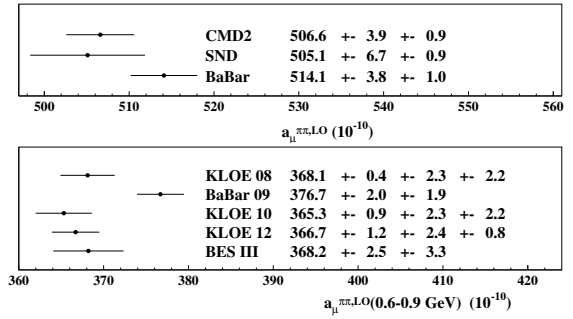


Figure 8: Measurements of $a_{\mu}^{\pi^+\pi^-}$: top, full energy range, adapted from [13]; bottom, (0.6 – 0.9 GeV), adapted from [19].

6 What about a_{μ} then ?

The time evolution of the prediction of a_{μ} with the availability of experimental results of increas-

Table 4: Summary of the *BABAR* results on ISR production of exclusive hadronic final states (The superseded results have been removed). Channels above the horizontal line have been mentioned in this paper.

Channels	$\int \mathcal{L} dt$ (fb $^{-1}$)	Method	Reference
$K_s^0 K^+ \pi^- \pi^0, K_s^0 K^+ \pi^- \eta$	454	LO	preliminary
$K^+ K^-$	469	LO, no tag	[44]
$K_s^0 K_L^0, K_s^0 K_L^0 \pi^+ \pi^-, K_s^0 K_s^0 \pi^+ \pi^-, K_s^0 K_s^0 K^+ K^-$	469	LO	[42]
$\bar{p} p$	454	LO	[43]
$\bar{p} p$	469	LO, no tag	[40]
$K^+ K^-$	232	NLO	[36]
$\pi^+ \pi^-$	232	NLO	[34] [35]
<hr/>			
$2(\pi^+ \pi^-)$	454	LO	[38]
$K^+ K^- \pi^+ \pi^-, K^+ K^- \pi^0 \pi^0, K^+ K^- K^+ K^-$	454	LO	[39]
$K^+ K^- \eta, K^+ K^- \pi^0, K^0 K^\pm \pi^\mp$	232	LO	[33]
$\pi^+ \pi^- \pi^0 \pi^0$	232	LO	[41] preliminary
$2(\pi^+ \pi^-) \pi^0, 2(\pi^+ \pi^-) \eta, K^+ K^- \pi^+ \pi^- \pi^0, K^+ K^- \pi^+ \pi^- \eta$	232	LO	[32]
$\Lambda \bar{\Lambda}, \Lambda \Sigma^0, \Sigma^0 \Sigma^0$	232	LO	[31]
$3(\pi^+ \pi^-), 2(\pi^+ \pi^- \pi^0), K^+ K^- 2(\pi^+ \pi^-)$	232	LO	[30]
$\pi^+ \pi^- \pi^0$	89	LO	[29]

Table 5: Comparison of $\pi^+ \pi^-$ data.

Experiment	Method	Norm	\sqrt{s} GeV	Systematics %	Reference
SND	scan	$\mathcal{L} + \text{MC}$	0.4 – 1.0	1.3	[21]
CMD2	scan	$\mathcal{L} + \text{MC}$	0.6 – 1.0	0.8	[20]
KLOE	ISR	$\mathcal{L} + \text{MC}$	0.592 – 0.975	0.9	[22]
BaBar	ISR	$\pi^+ \pi^- / \mu^+ \mu^-$	$2m_\pi c^2 - 3.0$	0.5 ^(a)	[34, 35]
KLOE	ISR	$\mathcal{L} + \text{MC}$	0.316 – 0.922	1.4	[23]
KLOE (1+2)	ISR	$\pi^+ \pi^- / \mu^+ \mu^-$	0.592 – 0.975	0.7	[24]
BES III	ISR	$\mathcal{L} + \text{MC}$	0.6 – 0.9	0.9	[19]

(a) In the range 0.6 – 0.9 GeV.

Table 6: e^+e^- - and τ -based values of a_μ^{VP} at the end of 2010 without [13] and with [15] $\rho-\gamma$ mixing taken into account. Beware the energy range on which the integral is performed differs.

	Davier <i>et al.</i> , [13] full energy range	Jegerlehner <i>et al.</i> , [15] 0.592 – 0.975 GeV
e^+e^-	692.3 ± 4.2	385.2 ± 1.6
τ	701.5 ± 4.7	386.0 ± 2.5
Δ	9.2 ± 6.3	0.8 ± 3.0

ing precision and with the development of combination techniques is shown in Fig. 7.

- For the $\pi^+ \pi^-$ channel, measurements with

the isospin mixed ($I = 0, 1$) $e^+e^- \rightarrow \pi^+ \pi^-$ have been complemented by measurements with the $I = 1$ $\tau^- \rightarrow \pi^- \pi^0 \nu_\tau$ (and c.c.) decay, after isospin breaking effects are corrected ([11] and references therein). τ -based predictions have long been larger than e^+e^- -based predictions.

After the fact that the $\rho-\gamma$ mixing that is present in $e^+e^- \rightarrow \pi^+ \pi^-$ and that is absent in the $\tau^- \rightarrow \pi^- \pi^0 \nu_\tau$ decay, is taken into account, the discrepancy between the combinations based on e^+e^- results and those based on the τ decay spectral functions [11] is resolved ([15] and Table 6).

- The discrepancy between the prediction and the measurement staying close to $3. \times 10^{-9}$ and the uncertainty improving with new measurements pouring in, the significance of the discrepancy has been increasing and almost reaches 4 standard deviations.
- Given that the precision of most measurements is now dominated by the systematics, I am not sure what the potential for major improvements at a super- B factory might be.
- Thanks to the high-precision results obtained up to the end of 2014, the uncertainty on a_μ^{VP} is now smaller than 4×10^{-10} [16]. That work includes a NNLO correction for a_μ^{VP} [17] and a NLO contribution to a_μ^{LbL} [18]. Given the spread of the values predicted by the available models of light-by-light scattering, the global uncertainty on a_μ^{LbL} is of the same order of magnitude [10, 16].
- Indeed, new measurements of a_μ at Fermilab [25] and at J-PARC [26] are eagerly awaited.

7 Acknowledgements

Many thanks to the fellow BaBarians who helped me to prepare this talk and to Fedor Ignatov who provided me with the *BABAR* summary plot (Fig. 6).

References

- [1] J. E. Nafe *et al.*, Phys. Rev. **71**, 914 (1947).
- [2] J.S. Schwinger, Phys. Rev. **73** (1948) 416.
- [3] T. Aoyama *et al.*, Phys. Rev. Lett. **109** (2012) 111808.
- [4] K. A. Olive *et al.* [Particle Data Group], Chin. Phys. C **38** (2014) 090001.
- [5] G. W. Bennett *et al.* [Muon g-2], Phys. Rev. D **73**, 072003 (2006).
- [6] G. Bonneau and F. Martin, Nucl. Phys. B **27**, 381 (1971).
- [7] A. J. Bevan *et al.* [BaBar and Belle], Eur. Phys. J. C **74**, 3026 (2014).
- [8] V. L. Chernyak, A. R. Zhitnitsky and V. G. Serbo, JETP Lett. **26**, 594 (1977) [Pisma Zh. Eksp. Teor. Fiz. **26**, 760 (1977)].
- [9] K. Hagiwara *et al.*, Phys. Lett. B **649**, 173 (2007).
- [10] F. Jegerlehner and A. Nyffeler, Phys. Rept. **477** (2009) 1.
- [11] M. Davier *et al.*, Eur. Phys. J. C **66** (2010) 127.
- [12] M. Davier *et al.*, Eur. Phys. J. C **66**, 1 (2010).
- [13] M. Davier *et al.*, Eur. Phys. J. C **71** (2011) 1515 [Erratum-ibid. C **72** (2012) 1874].
- [14] K. Hagiwara *et al.*, J. Phys. G **38** (2011) 085003.
- [15] F. Jegerlehner and R. Szafron, Eur. Phys. J. C **71** (2011) 1632.
- [16] F. Jegerlehner, arXiv:1511.04473 [hep-ph].
- [17] A. Kurz *et al.*, Phys. Lett. B **734**, 144 (2014).
- [18] G. Colangelo *et al.*, Phys. Lett. B **735**, 90 (2014).
- [19] M. Ablikim *et al.* [BESIII], Phys. Lett. B **753**, 629 (2016).
- [20] R. R. Akhmetshin *et al.* [CMD-2], Phys. Lett. B **648**, 28 (2007).
- [21] M. N. Achasov *et al.* [SND], J. Exp. Theor. Phys. **101**, 1053 (2005) [Zh. Eksp. Teor. Fiz. **101**, 1201 (2005)].
- [22] F. Ambrosino *et al.* [KLOE], Phys. Lett. B **670**, 285 (2009).
- [23] F. Ambrosino *et al.* [KLOE], Phys. Lett. B **700**, 102 (2011).
- [24] D. Babusci *et al.* [KLOE], Phys. Lett. B **720**, 336 (2013).
- [25] G. Venanzoni [Fermilab E989], Nucl. Phys. Proc. Suppl. **225** (2012) 277.
- [26] T. Mibe [J-PARC g-2], Nucl. Phys. Proc. Suppl. **218** (2011) 242.

The BaBar Collaboration:

- [27] Nucl. Instrum. Meth. A **479**, 1 (2002).
- [28] Nucl. Instrum. Meth. A **729**, 615 (2013).
- [29] $e^+e^- \rightarrow \pi^+\pi^-\pi^0$, Phys. Rev. D **70** (2004) 072004,
- [30] $e^+e^- \rightarrow 3(\pi^+\pi^-), 2(\pi^+\pi^-\pi^0)$ and $K^+K^-2(\pi^+\pi^-)$, Phys. Rev. D **73** (2006) 052003.
- [31] $e^+e^- \rightarrow \Lambda\bar{\Lambda}, \Lambda\bar{\Sigma}^0, \Sigma^0\bar{\Sigma}^0$, Phys. Rev. D **76** (2007) 092006.
- [32] $e^+e^- \rightarrow 2(\pi^+\pi^-)\pi^0, 2(\pi^+\pi^-)\eta, K^+K^-\pi^+\pi^-\pi^0$ and $K^+K^-\pi^+\pi^-\eta$, Phys. Rev. D **76** (2007) 092005 [Erratum-ibid. **77** (2008) 119902].

- [33] $e^+e^- \rightarrow K^+K^-\eta$, $K^+K^-\pi^0$ and $K_s^0K^\pm\pi^\mp$, Phys. Rev. D **77** (2008) 092002.
- [34] $e^+e^- \rightarrow \pi^+\pi^-(\gamma)$, Phys. Rev. Lett. **103** (2009) 231801.
- [35] $e^+e^- \rightarrow \pi^+\pi^-(\gamma)$, Phys. Rev. D **86** (2012) 032013.
- [36] $e^+e^- \rightarrow K^+K^-(\gamma)$, Phys. Rev. D **88** (2013) 032013.
- [37] “ISR interference in $e^+e^- \rightarrow \mu^+\mu^-\gamma$ and $e^+e^- \rightarrow \pi^+\pi^-\gamma$ ”, Phys. Rev. D **92**, 072015 (2015).
- [38] $e^+e^- \rightarrow \pi^+\pi^-\pi^+\pi^-$, Phys. Rev. D **85** (2012) 112009.
- [39] $e^+e^- \rightarrow K^+K^-\pi^+\pi^-$, $K^+K^-\pi^0\pi^0$, and $K^+K^-K^+K^-$, Phys. Rev. D **86** (2012) 012008.
- [40] $e^+e^- \rightarrow \bar{p}p$ from 3.0 to 6.5 GeV, Phys. Rev. D **88** (2013) 072009.
- [41] V. P. Druzhinin, LP07, Daegu, Korea, August 13-18 2007, arXiv:0710.3455 [hep-ex].
- [42] $e^+e^- \rightarrow K_S^0K_L^0$, $K_S^0K_L^0\pi^+\pi^-$, $K_S^0K_S^0\pi^+\pi^-$, and $K_S^0K_S^0K^+K^-$, Phys. Rev. D **89**, 092002 (2014).
- [43] $e^+e^- \rightarrow p\bar{p}$, Phys. Rev. D **87**, 092005 (2013).
- [44] “ $e^+e^- \rightarrow K^+K^-$ from 2.6 to 8.0 GeV”, Phys. Rev. D **92**, 072008 (2015).